Selective Leaching of Vanadium from Roasted Stone Coal by Dilute Sulfuric Acid Dephosphorization-Two-Stage Pressure Acid Leaching

Jun Huang [1,3], Yimin Zhang [1,2,3,*], Jing Huang [1,2,3], Tao Liu [1,2,3], Zhenlei Cai [1,2,3] and Nannan Xue [1,2]

[1]   College of Resources and Environmental Engineering, Wuhan University of Science and Technology, Wuhan 430081, China; 15972153558@163.com (J.H.); jing_huang81@126.com (J.H.); liutao781019@126.com (T.L.); caizhenlei@wust.edu.cn (Z.C.); cbdis@aliyun.com (N.X.)

[2]   Hubei Provincial Engineering Technology Research Center of High Efficient Cleaning Utilization for Shale Vanadium Resource, Wuhan 430081, China

[3]   Hubei Provincial Collaborative Innovation Center for High Efficient Utilization of Vanadium Resources, Wuhan 430081, China

*   Correspondence: zym126135@126.com; Tel.: +86-27-6886-2057

Abstract: A novel staged leaching process has been reported in this paper to selectively extract vanadium from roasted stone coal and the mechanisms have been clarified. Results showed that the leaching efficiency of V, Al, P and Fe was 80.46%, 12.24%, 0.67% and 3.12%, respectively, under the optimum dilute sulfuric acid dephosphorization (DSAD)-two-stage pressure acid leaching (PAL) conditions. The efficient separation of V from Fe, Al and P was realized. As apatite could be leached more easily than mica, the apatite could completely react with sulfuric acid, while the mica had almost no change in the DSAD process, which was the key aspect in realizing the effective separation of V from P. Similarly, the hydrolyzation of Fe and Al could be initiated more easily than that of V by decreasing the residual acid of leachate. The alunite and iron-sulphate compound generated in the first-stage PAL process resulted in the effective separation of V from Fe and Al.

1. Introduction

In China, the gross reserve of vanadium in stone coal was 118 million tons in the terms of V_2O_5 [1,2]. The vast amount of these deposits has made stone coal be of considerable interest as a vanadium source. As for the traditional vanadium extraction process from stone coal, the salt roasting-water leaching technology was already eliminated due to the low vanadium recovery and the serious environmental pollution [3]. Recently, the acid leaching process for vanadium extraction from stone coal after oxidizing roasting, which was efficient and environmental-friendly, has attracted increasing attention, and the pressure acid leaching (PAL) process, with advantages of higher recovery and shorter production cycle, has become the research hotspot in this area [4,5]. However, the impurities content in leachate is usually very high [6]. These impurities, particularly the Fe, Al and P, could decrease the recovery of vanadium in a series of ways: Fe will be accumulated in the D2EHPA/TBP (Bis(ethyl)-phosphonic acid/Tributyl phosphate) [7], which results in the reduction of solvent saturation capacity; Al will also be accumulated in the D2EHPA/TBP, which results in a sharp decrease of vanadium extraction ratios [8]; P will combine with vanadate ions to produce

heteropolyacid anions, which inhabits the precipitation of ammonium vanadates [9]. Therefore, it is urgent to solve the problem of selectively leaching vanadium from the roasted stone coal, which still remains a challenge in industrial operations.

The effective separation of valuable metals from impurities had been realized in many other fields by selective leaching technology. Xia studied the removal of phosphorus from high phosphorus iron ores by selective HCl leaching method and found that, under proper conditions, the removal rate of phosphorus could exceed 98% [10]. The removal of phosphorus from high phosphorus iron ores using acid leaching had also been investigated by Chen and Jin, and the high removal rate of phosphorus has been realized [11,12]. Their studies showed that it is possible to realize the effective separation of V from P by DSAD. On the other hand, Önal investigated the PAL of Çaldağ lateritic nickel ore and found that, under high temperature reaction conditions, the Fe and Al leached were re-precipitated as hematite and alunite respectively and decreasing the residual acid of leachate could accelerate the precipitation of Fe and Al [13]. For decreasing the residual acid of leachate, the two-stage PAL process was usually used and a good effect could be obtained [14]. Moreover, the two-stage acid leaching was also cost-effective due to the lower acid consumption [1]. Thus, it was possible to achieve the effective separation of V from Fe and Al by two-stage PAL.

In this study, the effect of sulfuric acid concentration and temperature on dephosphorization efficiency and vanadium loss has been studied. Then the effect of various factors such as the first-stage initial sulfuric acid concentration, the first-stage leaching temperature, the second-stage sulfuric acid concentration and the second-stage leaching temperature on the leaching of V, Fe, Al and P were studied. Finally, X-ray diffraction (XRD), X-ray photoelectron spectroscopy (XPS) and thermodynamics analysis were carried out to study the basic principles on the selective leaching of vanadium from roasted stone coal.

2. Experimental

2.1. Materials

In this work the stone coal was obtained from Tongshan located in Hubei Province, China. The raw ore was crushed to −3 mm and it was roasted in a SXZ-10-B muffle furnace (Shanghai Experimental Furnace Plant, Shanghai, China) at 850 °C for 60 min and then dry ground to 80% −0.074 mm in size with a XZM-100 vibration mill (Wuhan Hengyue Mineral Engineering Company, Wuhan, China). The roasted and gained ore was referred to as the roasted stone coal throughout this work.

The main chemical composition of roasted stone coal was analyzed by inductively coupled plasma atomic emission spectroscopy (ICP-AES) (Thermo Scientific, Waltham, MA, USA) listed in Table 1. It was indicated that the composition of roasted stone coal was complex. The roasted stone coal was mainly composed of quartz, hematite, gypsum, calcite and mica (Figure 1). The vanadium that existed in mica was mainly in the form of lattice replacement according to the study of Zhang [15]. The quantitative evaluation of minerals by scanning electron microscopy (QEMSCAN) analysis (FEI, Hillsboro, OR, USA) (Figure 2) of roasted stone coal showed that there were small amounts of apatite existed in this roasted stone coal and the apatite was the only source of P.
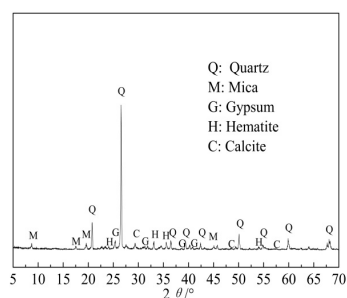

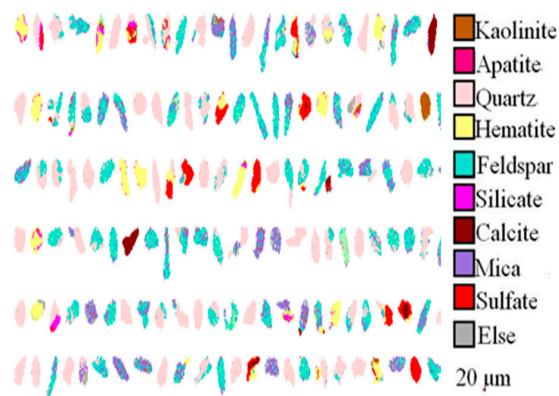**Figure 1.** X-ray diffraction (XRD) pattern for roasted stone coal.

Figure 2. Quantitative evaluation of minerals by scanning electron microscopy (QEMSCAN) analysis result for the stone coal roasted residue.

Table 1. Main chemical composition of the stone coal roasted residue (wt %).

Element	SiO_2	CaO	Al_2O_3	V_2O_5	Fe_2O_3	K_2O	Na_2O	MgO	P_2O_5
Content	66.0	5.29	9.81	0.83	4.96	2.51	0.30	1.67	1.03

All the reagents used in this study were of analytical reagent grade and the water used was distilled water.

2.2. Experimental Procedure

The experiments were preformed according to the flow sheet as show in Figure 3. According to our previous study, all of these tests were conducted at the liquid-to-solid ratio of 1.5 mL/g (the volume/mass ratio of dilute sulfuric acid to raw ore) for 120 min [16].
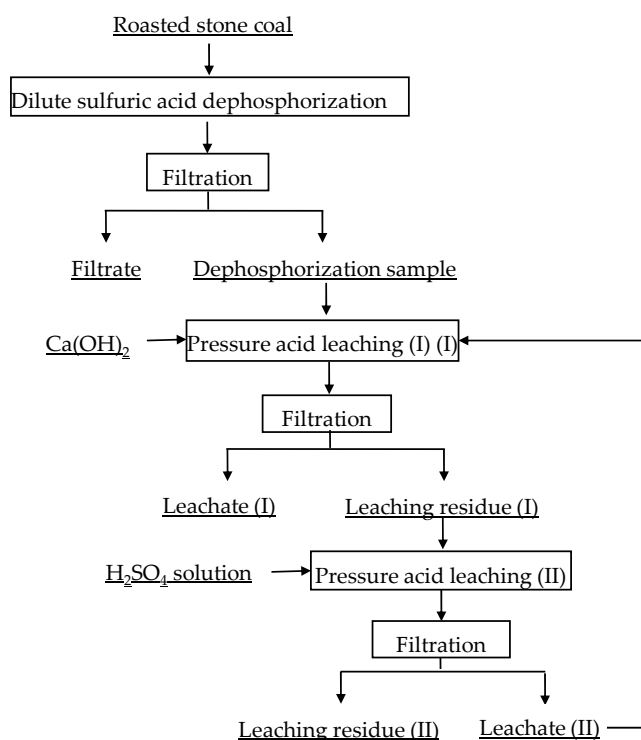

Figure 3. Flow sheet of the dilute sulfuric acid dephosphorization (DSAD)-two-stage pressure acid leaching (PAL) process.

2.2.1. DSAD Test

In order to achieve the effective separation of V from P, the DSAD tests were conducted. In this process the roasted stone coal was leached in a SZCL-2A magnetic and controlling temperature stirrer (Wuhan Keer Instrument Company, Wuhan, China). The sulfuric acid concentration was 1.0% (v/v), 1.5% (v/v), 2.0% (v/v), 2.5% (v/v), 3.0% (v/v), 3.5% (v/v) and 4.0% (v/v) and the temperature was controlled at 20, 40, 60, 80 and 100 °C. After DSAD process, the slurries were filtrated by SHB-III vacuum suction filter device (Wuhan Keer Instrument Company, Wuhan, China). Then the contents of V and P in filtrate were analyzed.

2.2.2. Two-Stage PAL Test

For achieving the effective separation of V from Fe and Al, the two-stage PAL tests were carried out.

In the first-stage PAL process the dephosphorization sample was leached by leachate (II) in a GSH-2 autoclave (Weihai Shandong Chaoyang Chemical Machinery Co., Ltd., Weihai, China) at the liquid-to-solid ratio of 1.5 mL/g, the leaching time of 120 min and the total pressure of 1.0 MPa. The first-stage sulfuric acid concentration was adjusted to 2.50% (v/v), 3.75% (v/v), 4.50% (v/v), 6.00% (v/v), 7.50% (v/v) by adding $Ca(OH)_2$ and the temperature was controlled at 90, 120, 150, 180 and 210 °C, respectively. After the first-stage PAL the slurries were filtrated and then the contents of V, Fe, Al and P in leachate (I) were analyzed. Leaching residue (I) was leached by H_2SO_4 solution in the second-stage PAL process which was performed in a GSH-2 autoclave (Weihai Shandong Chaoyang Chemical Machinery Co., Ltd., Weihai, China) at the liquid-to-solid ratio of 1.5 mL/g, the leaching time of 120 min and the total pressure of 1.0 MPa. In this process, the second-stage sulfuric acid concentration was 7.5% (v/v), 10.0% (v/v), 12.5% (v/v), 15% (v/v), 17.5% (v/v) and 20.0% (v/v), and the temperature was controlled at 90, 120, 150, 180 and 210 °C, respectively. After the second-stage PAL the slurries were filtrated. The leachate (II) was returned to the first-stage leaching for utilizing the residual sulfuric acid. After recycling the leachate (II) seven times the equilibrium result was obtained.

2.3. Analysis Methods

(1) The determination of vanadium content was measured in accordance with Test Methods of Vanadium in Coal Standard (GB/T 19226-2003) [16]. Other elements in this study were analyzed by using ICP-AES method which was conducted by an inductively coupled plasma-atomic emission spectrometer (Thermo Scientific) Advantage ER/S inductively coupled plasma-optical emission spectrometer (Thermo Scientific).

(2) The residual sulfuric acid concentration in leachate was determined by titration using 0.1 mol/L Na_2CO_3 solution with methyl orange as an indicator [17].

(3) XRD analysis was conducted by an Xpertpro X-ray diffractometer (D/MAX 2500PC, Rigaku, Tokyo, Japan) with Cu-Kα radiation, voltage 40 kV, current 30 mA and at the scanning rate of $15°\cdot min^{-1}$ from 5° to 70°.

(4) Detailed mineralogy on the roasted stone coal was done using quantitative evaluation of minerals by QEMSCAN analysis which was conducted by the QEMSCAN analysis system (FEI).

(5) The chemical species was analyzed by using a VG Multilab 2000 X-ray photoelectron spectrometer (Thermo Scientific) and an Al-Kα X-ray source with a solution of 0.47 eV.

3. Results and Discussion

3.1. The DSAD-Two-Stage PAL Result

3.1.1. DSAD Result

Figure 4a reported the dephosphorization efficiency and the vanadium loss obtained by varying sulfuric acid concentration. It can be seen that the dephosphorization efficiency apparently increased

to 98.75% with the sulfuric acid concentration increased to 3.0% (v/v). Further increase of the sulfuric acid concentration had only a slight effect on dephosphorization efficiency. Hence, the sulfuric acid concentration should be 3.0% (v/v).
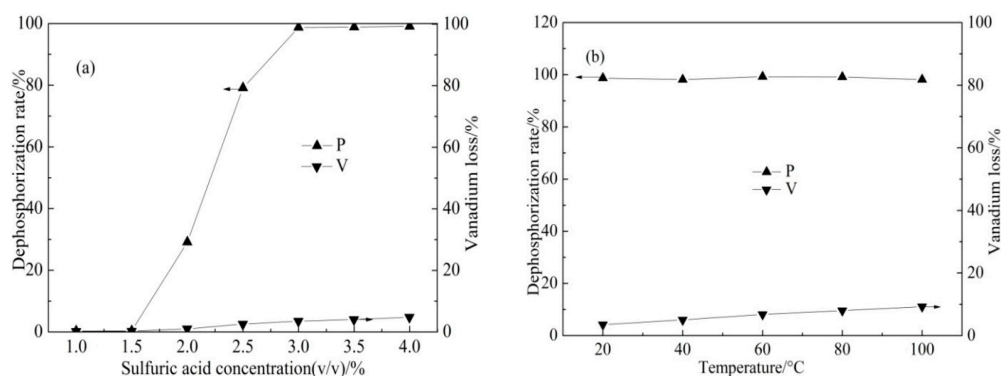

Figure 4. Effects of sulfuric acid concentration (**a**); and temperature (**b**) on the dephosphorization rate and the vanadium loss rate.

The effect of temperature on dephosphorization efficiency and vanadium loss were studied. The results (Figure 4b) showed that the vanadium loss increased from 3.52% to 9.25% with the increase of the temperature from 20 to 100 °C. However, the dephosphorization efficiency changed a little with the increase of the temperature. So the temperature was controlled at 20 °C in this study.

As discussed above, under these conditions that the temperature of 20 °C, the sulfuric acid concentration of 3.0% (v/v), the liquid/solid ratio of 1.5 mL/g, and the time of 120 min, the dephosphorization rate could reach 98.75% and the vanadium loss was just 3.52%, the dephosphorization effect was significant.

3.1.2. Pressure Acid Leaching (I) Result

According to the research of Rubisov [18], the higher the residual acid concentration in leachate, the more Fe and Al could be leached under these PAL conditions. Thus, the Ca(OH)$_2$ was added into pressure acid leaching (I) to decrease the residual sulfuric acid concentration of leachate (I). It was showed that both the residual sulfuric acid concentration and the leaching efficiency of Fe and Al decreased with the decrease of the initial sulfuric acid concentration of the first stage (Figure 5a). However, there was a sharp decrease in the leaching efficiency of V from 80.46% to 66.76% with the decrease in the first-stage initial sulfuric acid concentration from 3.75% (v/v) to 2.5% (v/v). Therefore, the optimum initial sulfuric acid concentration of the first stage was determined as 3.75% (v/v).
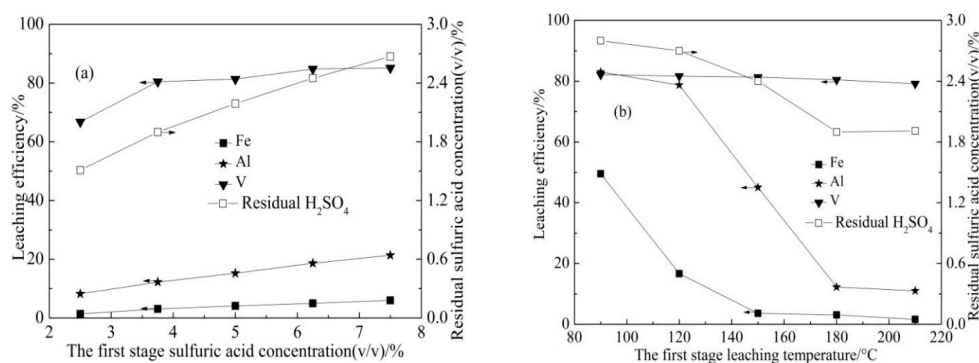

Figure 5. Effects of the acid pressure leaching (I) parameters on leaching efficiency of V, Al, P, Fe. (**a**) The initial sulfuric acid concentration of the first stage; (**b**) the leaching temperature of the first stage.

Figure 5b showed that the leaching efficiency of Fe and Al decreased sharply with the increase of the leaching temperature of the first stage from 90 to 180 °C. When the temperature was over 180 °C, the leaching efficiency of Fe, Al and V remains unchanged. Therefore, the first-stage leaching temperature was recommended as 180 °C and the leaching efficiency of V, Fe and Al was obtained as 80.46%, 3.12% and 12.24%, respectively.

3.1.3. Pressure Acid Leaching (II) Result

It was indicated that the leaching efficiency of V increased with the increase of the second-stage sulfuric acid concentration. When sulfuric acid concentration of the second stage was over 15% (*v*/*v*), the leaching efficiency of V slowly increased (Figure 6a). Therefore, the second-stage sulfuric acid concentration of 15% (*v*/*v*) was utilized in this study.
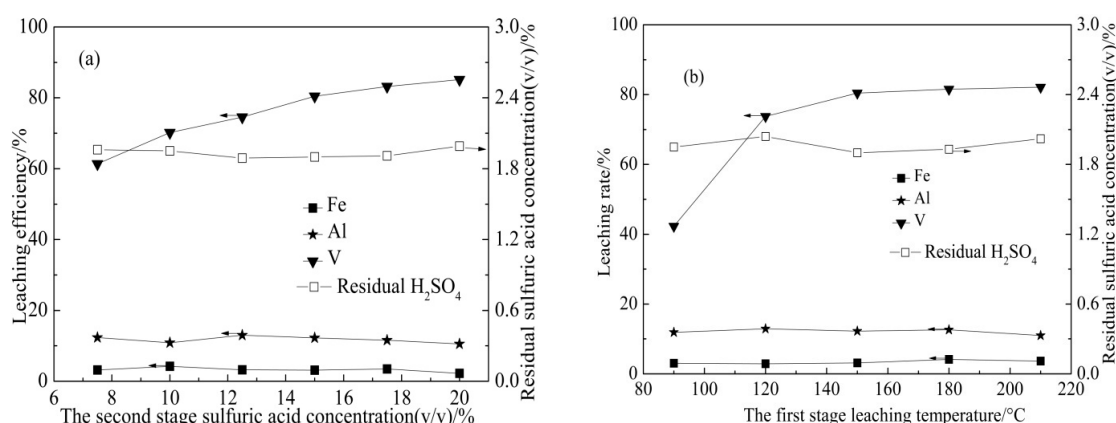

Figure 6. Effects of the acid pressure leaching (II) parameters on leaching efficiency of V, Al, P, Fe. (**a**) The sulfuric acid concentration of the second stage; (**b**) the leaching temperature of the second stage.

It was shown that, by increasing the leaching temperature of the second stage from 90 to 150 °C, the V leaching efficiency increased from 42.31% to 80.46%. Upon further increase of the leaching temperature of the second stage, the leaching efficiency of V, Fe and Al changed a little (Figure 6b). Thus, 150 °C was chosen as the optimal leaching temperature of the second stage in this study.

Therefore, the optimal conditions for the two-stage PAL were as follows: the liquid/solid ratio of 1.5 mL/g, the leaching time of 120 min, the leaching pressure of 1.0 MPa, the first-stage initial sulfuric acid concentration of 3.75% (*v*/*v*), the first-stage leaching temperature of 180 °C, the second-stage sulfuric acid concentration of 15% (*v*/*v*), the second-stage leaching temperature of 150 °C. The leaching efficiency of V, Al and Fe was 80.46%, 12.24% and 3.12%, respectively. Under these conditions, the leaching efficiency of P was just 0.67% (Table 2). Compared to the conventional PAL (i) and (ii), both the residual H_2SO_4 concentration and the leaching efficiency of Fe, Al and P has been significantly decreased (Table 2).

Table 2. Effect of leaching process on the residual H_2SO_4 concentration and leaching efficiencies of V, Fe, Al and P from the roasted stone coal (%).

Process	V	Fe	Al	P	Residual H_2SO_4 (*v*/*v*)
[a] Conventional PAL (i)	80.51	18.92	79.25	99.21	4.39
[b] Conventional PAL (ii)	82.13	19.96	60.48	98.20	4.29
[c] DSAD-two-stage PAL	80.46	3.12	12.24	0.67	1.90

Note: [a] Conventional PAL (i) was conducted with roasted stone coal in 15 % (*v*/*v*) H_2SO_4, liquid/solid ratio of 1.5 mL/g at 150 °C, 1.0 MPa for 120 min; [b] Conventional PAL (ii) was conducted with roasted stone coal in 15 % (*v*/*v*) H_2SO_4, liquid/solid ratio of 1.5 mL/g at 180 °C, 1.0 MPa for 120 min; [c] DSAD-two-stage PAL was conducted with roasted stone coal under the optimum conditions.

3.2. Analysis of Leaching Residue and Leachate

In order to investigate the main reactions of Fe, Al and P species in these processes, each stage residue was analyzed by XRD (Figure 7) and each stage filtrate was analyzed by ICP-AES (Table 3).
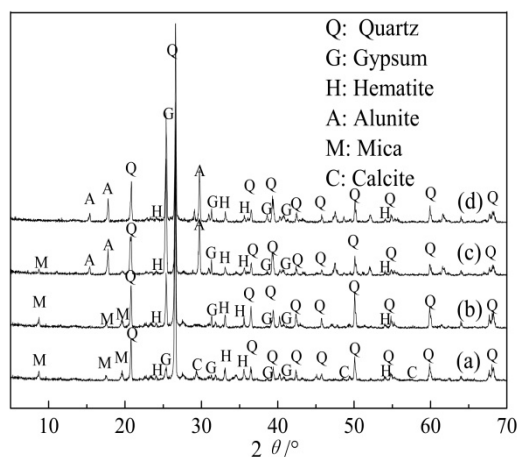

Figure 7. The XRD patterns for roasted stone coal (**a**); dephosphorization sample (**b**); leaching residue (I) (**c**); and leaching residue (II) (**d**).

Table 3. Content of V, Fe, Al and P for each stage filtrate (mg/L).

Each Stage Filtrate	V	Fe	Al	P
Filtrate	94	58	120	2864
Leachate (I)	2163	623	3672	19
Leachate (II)	1487	10019	20532	22

Compared with the intensity of mica peaks of roasted stone coal (curve (a) in Figure 7), the intensity of mica peaks of dephosphorization sample (curve (b) in Figure 7) had almost no changes, indicating that the mica has almost not dissolved in the DSAD process, which resulted in the low vanadium loss (Figure 4).

The XRD analysis of leaching residue (I) (curve (c) in Figure 7) showed that the peaks of alunite appeared in the first-stage PAL process. Accordingly, the content of Al in leachate decreased from 20,532 to 3672 mg/L (Table 3). These phenomena show that the alunite formed by Al hydrolysis was the controlling solid balancing of Al concentration in leachate (I). According to the research of Rubisov [18], increasing reaction temperature or decreasing residual acidity could promote the hydrolysis of Al at these PAL conditions with the result that lower leaching efficiency of Al was obtained (Figure 5).

It was indicated that the residual mica of leaching residue (I) completely dissolved in the second-stage PAL process (curve (c) and (d) in Figure 7), which was the key to realizing the effective leaching of V. According to the study of Li [5], increasing leaching temperature and acidity could promote the dissolution of mica, which resulted in the increase of vanadium leaching efficiency (Figure 6).

In order to further reveal the main reactions of Fe, Al and P species in these processes from the surface chemistry perspective, the XPS analysis was conducted in the binding energy regions of P 2p, Ca 2p, Fe 2p and Al 2p (Figure 8).
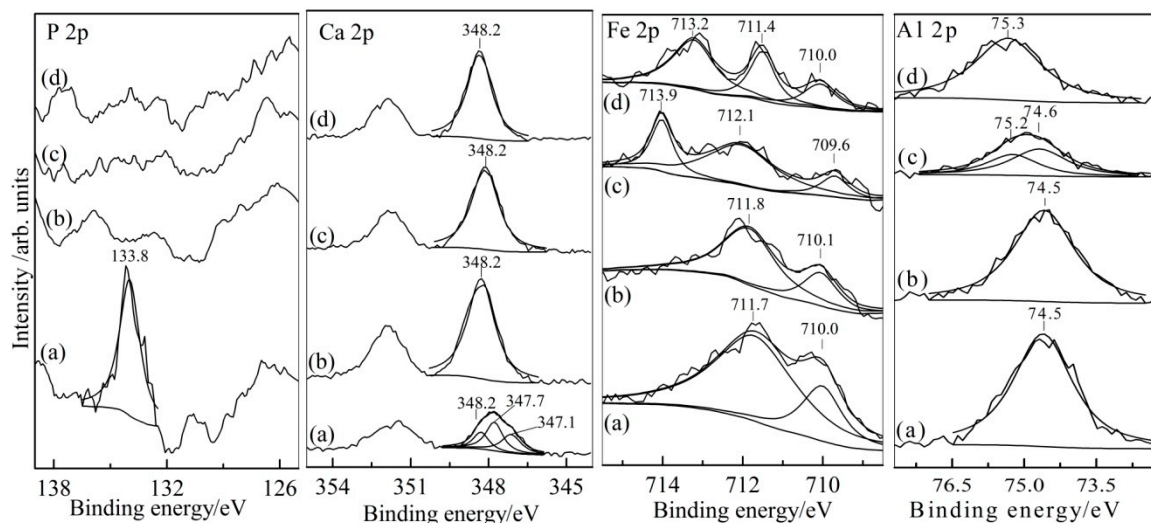
Figure 8. X-ray photoelectron P 2p, Ca 2p, Fe 2p and Al 2p spectra from roasted stone coal (**a**); dephosphorization sample (**b**); leaching residue (I) (**c**); and leaching residue (II) (**d**).

The P 2p spectrum could be fitted to the peak at 133.8 eV, which was the characteristic of pentavalent phosphorous in PO_4 tetrahedra (curve (a) in Figure 8) [19]. The raw Ca 2p spectrum was composed of three fitted curves. The binding energy at 347.1, 347.7 and 348.2 eV was the XPS peaks of Ca $2p_{3/2}$ for calcite, apatite and gypsum, respectively (curve (a) in Figure 8) [20–22]. After DSAD, the peaks at 133.8, 347.1 and 347.7 eV disappeared. However, the peak at 348.2 eV became stronger, which suggested that the apatite and calcite had already completely reacted with sulfuric acid in the DSAD process. This was the key to achieving the high dephosphorization rate.

The Fe 2p XPS spectrums in Figure 8a–d showed two peaks near 711.7 and 710.0 eV corresponding to hematite and magnetite [23], respectively. After the first-stage PAL, a new peak around 713.6 eV corresponding to Fe $2p_{3/2}$ for Fe-SO_4 appeared [24,25]. It was suggested that a new kind of iron-sulphate compound generated, which resulted in the decrease of Fe concentration from 10,019 to 623 mg/L (Table 3). According to the recent published paper [26], this iron-sulphate compound generated by Fe hydrolyzation was probably the schwertmannite $Fe_8O_8(OH)_6SO_4$, a jarosite precursor phase, and increasing reaction temperature or decreasing residual acidity could promote the formation of schwertmannite, which resulted in the lower leaching efficiency of Fe (Figure 5). After the first-stage PAL, the peaks' intensity of hematite became smaller (curve (b) and (c) in Figure 7). It was suggested that the hematite partly dissolved. The generation of iron-sulphate compound and the dissolution of hematite in the first-stage PAL process indicated that the formation of iron-sulphate compound by Fe hydrolyzation could be initiated more easily than that of hematite under these pressure acid leaching conditions, because the strong binding anions like SO_4^{2-} could favor the formation of this iron-sulphate compound [27].

The Al 2p XPS peak centered at 74.5 eV assigned to mica [28] had almost no change in the DSAD process (curve (a) and curve (b) in Figure 8). It is suggested that the mica structure has not been destroyed. After the first-stage PAL, another peak centered at 75.3 eV assigned to Al-SO_4 bonds [29] appeared. This phenomenon was consistent with the generation of alunite (curve (b) and (c) in Figure 7). After the second-stage PAL, the peak of mica disappeared, which suggested that the mica has completely dissolved, which was in accordance with the XRD analysis result (curve (c) and (d) in Figure 7). The presence of alunite and the absence of mica reflected that the alunite was more difficult to leach than mica.

3.3. Thermodynamics Analysis

In order to achieve a better understanding of the principles of selective leaching of V from roasted stone coal by DSAD-two-stage PAL, thermodynamics was applied into the analysis. As discussed above, it was inferred that the possible main equilibrium reactions in these processes could be described as Equations (1)–(20) in Table 4. The Equations (21)–(29) were equilibrium reactions of the species involved in Equations (1)–(20) [30]. All of these equilibrium reactions could be expressed as Formula (1).

$$a\text{A} + n\text{H}^+ = b\text{B} + c\text{H}_2\text{O} \tag{1}$$

Table 4. pH_T^θ of different equilibrium reactions at 373–473 K.

Number	Equilibrium Reaction	pH_{273}^θ	pH_{323}^θ	pH_{373}^θ	pH_{423}^θ	pH_{473}^θ
1	$CaCO_3 + HSO_4^- + H^+ = CO_2\uparrow + CaSO_4\downarrow + H_2O$	13.23	12.53	12.14	11.95	11.91
2	**$CaCO_3 + SO_4^{2-} + 2H^+ = CO_2\uparrow + CaSO_4\downarrow + H_2O$**	**7.43**	**7.40**	**7.58**	**7.87**	**8.25**
3	$CaCO_3 + SO_4^{2-} + H^+ = CaSO_4\downarrow + HCO_3^-$	7.17	6.81	6.79	6.95	7.26
4	**$Fe_2O_3 + 6H^+ = 2Fe^{3+} + 3H_2O$**	**0.49**	**−0.16**	**−0.65**	**−1.03**	**−1.36**
5	**$KAl_2(AlSi_3O_{10})(OH)_2 + 10H^+ = 3Al^{3+} + K^+ + 3H_4SiO_4$**	**2.20**	**1.35**	**0.72**	**0.22**	**−0.20**
6	$KAl_2(AlSi_3O_{10})(OH)_2 + 7H^+ = 3Al^{3+} + K^+ + 3HSiO_3^- + 3H_2O$	−1.90	−2.65	−3.30	−3.89	−4.46
7	**$KAl_3(SO_4)_2(OH)_6 + 8H^+ = 3Al^{3+} + K^+ + 2HSO_4^-$**	**1.07**	**0.38**	**−0.21**	**−0.74**	**−1.24**
8	$KAl_3(SO_4)_2(OH)_6 + 6H^+ = 3Al^{3+} + 6H_2O + K^+ + 2SO_4^{2-}$	0.89	−0.24	−1.29	−2.25	−3.18
9	$Ca_5(PO_4)_3F + 2H^+ + 5HSO_4^- = 5CaSO_4\downarrow + 3H_2PO_4^- + HF$	6.88	5.22	3.99	3.05	2.34
10	$Ca_5(PO_4)_3F + 5H^+ + 5HSO_4^- = 5CaSO_4\downarrow + 3H_3PO_4 + HF$	0.63	0.41	0.50	0.67	0.92
11	$Ca_5(PO_4)_3F + H^+ + 5SO_4^{2-} = 5CaSO_4\downarrow + 3PO_4^{3-} + HF$	−37.99	−36.35	−35.16	−34.29	−33.67
12	$Ca_5(PO_4)_3F + 4H^+ + 5SO_4^{2-} = 5CaSO_4\downarrow + 3HPO_4^{2-} + HF$	−0.02	0.05	0.28	0.58	0.94
13	$Ca_5(PO_4)_3F + 7H^+ + 5SO_4^{2-} = 5CaSO_4\downarrow + 3H_2PO_4^- + HF$	3.13	3.11	3.30	3.58	3.95
14	$Ca_5(PO_4)_3F + 10H^+ + 5SO_4^{2-} = 5CaSO_4\downarrow + 3H_3PO_4 + HF$	1.13	1.34	1.76	2.23	2.75
15	$Ca_5(PO_4)_3F + H^+ + 5HSO_4^- = 5CaSO_4\downarrow + 3H_2PO_4^- + F^-$	10.79	7.12	4.28	2.03	0.21
16	$Ca_5(PO_4)_3F + 4H^+ + 5HSO_4^- = 5CaSO_4\downarrow + 3H_3PO_4 + F^-$	0.04	−0.32	−0.30	−0.18	0.03
17	$Ca_5(PO_4)_3F + 3H^+ + 5SO_4^{2-} = 5CaSO_4\downarrow + 3HPO_4^{2-} + F^-$	−1.02	−1.04	−0.86	−0.58	−0.24
18	**$Ca_5(PO_4)_3F + 6H^+ + 5SO_4^{2-} = 5CaSO_4\downarrow + 3H_2PO_4^- + F^-$**	**6.30**	**6.16**	**6.46**	**6.99**	**7.71**
19	$Ca_5(PO_4)_3F + 9H^+ + 5SO_4^{2-} = 5CaSO_4\downarrow + 3H_3PO_4 + F^-$	0.92	1.12	1.54	2.02	2.56
20	**$V_2O_4 + 4H^+ = 2VO^{2+} + 2H_2O$**	**2.62**	**1.74**	**1.14**	**0.70**	**0.36**
21	$SO_4^{2-} + H^+ = HSO_4^-$	1.62	2.27	3.02	3.79	4.59
22	$HSiO_3^- + H^+ + H_2O = H_4SiO_4$	11.80	10.69	10.10	9.82	9.76
23	$SiO_4^{4-} + 3H^+ = HSiO_3^- + H_2O$	13.68	12.90	12.72	12.95	13.43
24	$HCO_3^- + H^+ = CO_2\uparrow + H_2O$	7.68	7.99	8.36	8.78	9.24
25	$CO_3^{2-} + H^+ = HCO_3^-$	10.62	10.17	10.09	10.22	10.51
26	$F^- + H^+ = HF$	2.98	3.33	3.70	4.07	4.48
27	$H_2PO_4^- + H^+ = H_3PO_4$	−3.54	−2.80	−1.83	−0.92	−0.04
28	$HPO_4^{2-} + H^+ = H_2PO_4^-$	7.32	7.19	7.32	7.58	7.95
29	$PO_4^{3-} + H^+ = HPO_4^{2-}$	12.64	12.19	12.09	12.21	12.48

The Gibbs free energy change of reaction Formula (1) could be calculated as Formula (2).

$$\Delta_r G_T = \Delta_r G_T^\theta + RT\ln\frac{a_B^b}{a_A^a} + 2.303nRT\text{pH}_T \tag{2}$$

For dissolving A, the Gibbs free energy change should satisfy that: $\Delta_r G_T \leqslant 0$. Formula (2) could transform to Formula (3).

$$\text{pH}_T \leqslant \frac{-\Delta_r G_T^\theta}{2.303nRT} + \frac{1}{n}\lg\frac{a_B^b}{a_A^a} \tag{3}$$

For simplifying calculation, the activities of all species involved in the reactions have been considered to be 1, i.e., $a_A = a_B = 1$. The Formula (3) could transform to Formula (4)

$$\text{pH}_T \leqslant \text{pH}_T^\theta = \frac{-\Delta_r G_T^\theta}{2.303nRT} \tag{4}$$

The Gibbs free energy data required at high temperature were obtained from the research of Yang [31], and then the pH_T^θ values of these reactions calculated (Table 4) as Formula (4) [32]. It was indicated that the lower the pH_T^θ values was, the easier the A could be leached.

The theoretical equilibrium reactions of minerals in sulfuric acid solution were determined by the following methods: for the equation 1 in which CO_2 and HSO_4^- involved, this equation should balance in the stable region of CO_2 and HSO_4^- (according to the Equations (21)–(29), CO_2 and HSO_4^- exist in the acid solution of pH < pH_T^θ (24) and pH < pH_T^θ (21), respectively), i.e., the pH_T^θ of Equation (1) should be lower than that of Equations (21) and (24). However, the calculated result was inconsistent with this (Table 4). Thus, Equation (1) was not the equilibrium reaction of calcite in sulfuric acid solution. With this method, the Equation (2) was determined as theoretical equilibrium reaction of calcite in sulfuric acid solution. Similarly, the theoretical equilibrium reactions of hematite, mica, alunite, apatite and V_2O_4 in sulfuric acid solution were determined as Equations (4), (5), (7), (18) and (20), respectively.

According to the calculated results of Equations (4), (5), (7), (18) and (20), the pH_T^θ value of these minerals were in this order: calcite > apatite > mica > alunite > hematite (Table 4). Therefore, the difficult degree sequences of leaching could be inferred as follows: hematite > alunite > mica > apatite > calcite. As apatite could be leached more easily than mica, the apatite could completely reacted with sulfuric acid while the mica almost has no change in the DSAD process which was the key to achieving the effective separation of V from P. Table 4 also showed that the pH_T^θ value of V_2O_4 was higher than that of hematite and alunite, i.e., the difficult degree sequences of hydrolyzation could be inferred as follows: V_2O_4 > alunite > hematite. According to the former analysis, the formation of the iron-sulphate compound by Fe hydrolyzation could be initiated more easily than that of hematite under these leaching conditions. Therefore, the conclusion could be obtained that the hydrolyzation of Fe and Al could be initiated more easily than that of V by decreasing the residual acid of leachate, which was the key to achieving the effective separation of V from Fe and Al. This explained very well that the Fe and Al concentration decreased greatly but the V concentration had not decreased after the first-stage PAL (Table 3).

4. Conclusions

From the results of this study, the following conclusions could be drawn:

(1) The selective leaching of vanadium from roasted stone coal could be realized by DSAD-two-stage PAL. The optimum DSAD conditions were: the temperature of 20 °C, the sulfuric acid concentration of 3.0% (*v/v*), the liquid/solid ratio of 1.5 mL/g and the time of 120 min. Under these DSAD conditions, the dephosphorization rate could reach 98.75%, while the vanadium loss rate was just 3.52%. After the DSAD, the effective separation of V from P was realized. Then the dephosphorization sample was treated by two-stage PAL with these conditions that the liquid/solid ratio of 1.5 mL/g, the leaching time of 120 min, the leaching pressure of 1.0 MPa, the first-stage sulfuric acid concentration of 3.75% (*v/v*), the first-stage leaching temperature of 180 °C, the second-stage sulfuric acid concentration of 15% (*v/v*), the second-stage leaching temperature of 150 °C. The leaching efficiency of V, Al, P, and Fe was 80.46%, 12.24%, 0.67% and 3.12%, respectively. After the two-stage PAL, the effective separation of V from Al and Fe was realized.

(2) The mechanisms of selective leaching of vanadium from roasted stone coal by DSAD-two-stage PAL could be described as follows: the apatite could be leached more easily than mica. Thus, the apatite could completely reacted with sulfuric acid while the mica almost had no change in the DSAD process, which was the key to achieving the effective separation of V from P. Similarly, as the hydrolyzation of Fe and Al could be initiated more easily than that of V by decreasing the residual acid of leachate, the alunite and the iron-sulphate compound were generated in the first-stage PAL process, which resulted in the effective separation of V from Fe and Al.

Author Contributions: Jun Huang, Jing Huang and Yimin Zhang conceived and designed the experiments. Jun Huang and Nannan Xue prepared the samples and performed the experiments. Jun Huang, Zhenlei Cai and

Jing Huang analyzed the data. Jun Huang, Yimin Zhang, Jing Huang and Tao Liu contributed to the writing and revising of the paper.

Conflicts of Interest: The authors declare no conflict of interest.

References

1. Zhang, Y.M.; Bao, S.X.; Liu, T.; Chen, T.J.; Huang, J. The technology of extracting vanadium from stone coal in China: History, current status and future prospects. *Hydrometallurgy* **2011**, *109*, 116–124. [CrossRef]
2. Cai, Z.L.; Zhang, Y.M.; Liu, T.; Huang, J. Mechanisms of vanadium recovery from stone coal by novel BaCO$_3$/CaO composite additive roasting and acid leaching technology. *Minerals* **2016**, *6*, 26. [CrossRef]
3. Wang, L.; Sun, W.; Liu, R.Q.; Gu, X.C. Flotation recovery of vanadium from low-grade stone coal. *Trans. Nonferrous Met. Soc. China* **2014**, *24*, 1145–1151. [CrossRef]
4. Zhou, X.Y.; Li, C.L.; Li, J.; Liu, H.Z.; Wu, S.Y. Leaching of vanadium from carbonaceous shale. *Hydrometallurgy* **2009**, *99*, 97–99. [CrossRef]
5. Li, M.T.; Wei, C.; Qiu, S.; Zhou, X.J.; Li, C.X.; Deng, Z.G. Kinetics of vanadium dissolution from black shale in pressure acid leaching. *Hydrometallurgy* **2010**, *104*, 193–200. [CrossRef]
6. Li, X.B.; Wei, C.; Deng, Z.G.; Li, M.T.; Li, C.X.; Fan, G. Selective solvent extraction of vanadium over iron from stone coal/black shale acid leach solution by D2EHPA/TBP. *Hydrometallurgy* **2011**, *105*, 359–363. [CrossRef]
7. Ma, Y.Q.; Wang, X.W.; Wang, M.Y.; Jiang, C.J.; Xiang, X.Y.; Zhang, X.L. Separation of V(IV) and Fe(III) from the acid leach solution of stone coal by D2EHPA/TBP. *Hydrometallurgy* **2015**, *153*, 38–45. [CrossRef]
8. Li, W.; Zhang, Y.M.; Liu, T.; Huang, J.; Wang, Y. Comparison of ion exchange and solvent extraction in recovering vanadium from sulfuric acid leach solutions of stone coal. *Hydrometallurgy* **2013**, *131–132*, 1–7. [CrossRef]
9. Li, H.Y.; Wang, K.; Hua, W.H.; Yang, Z.; Zhou, W.; Xie, B. Selective leaching of vanadium in calcification-roasted vanadium slag by ammonium carbonate. *Hydrometallurgy* **2016**, *160*, 18–25. [CrossRef]
10. Xia, W.T.; Ren, Z.D.; Gao, Y.F. Removal of phosphorus from high phosphorus iron ores by selective HCl leaching method. *J. Iron Steel Res. Int.* **2011**, *18*, 1–4. [CrossRef]
11. Chen, C.Y.; Misra, V.N.; Clough, J.; Mun, R. Dephosphorisation of western Australian iron ore by hydrometallurgical process. *Miner. Eng.* **1999**, *12*, 1083–1092. [CrossRef]
12. Jin, Y.S.; Jiang, T.; Yang, Y.B.; Li, Q.; Li, G.H.; Guo, Y.F. Removal of phosphorus from iron ores by chemical leaching. *J. Cent. South. Univ. Technol.* **2006**, *13*, 673–677. [CrossRef]
13. Önal, M.A.R.; Topkaya, Y.A. Pressure acid leaching of Çaldağ lateritic nickel ore: An alternative to heap leaching. *Hydrometallurgy* **2014**, *142*, 98–107. [CrossRef]
14. Xu, B.; Zhong, H.; Jiang, T. Recovery of valuable metals from Gacun complex copper concentrate by two-stage countercurrent oxygen pressure acid leaching process. *Miner. Eng.* **2011**, *24*, 1082–1083. [CrossRef]
15. Zhang, Y.M.; Zhu, X.B.; Liu, T.; Huang, J.; Song, S.X. Effect of colloidal potassium alum formation on vanadium recovery from acid leach solutions of stone coal. *Hydrometallurgy* **2013**, *13*, 54–58. [CrossRef]
16. Huang, J.; Zhang, Y.M.; Huang, J.; Liu, T.; Xue, N.N. Study on Roasting-Pressure Acid Leaching of Vanadium from Stone Coal. *Metal Mine* **2015**, *10*, 85–89. (In Chinese)
17. Li, W.; Zhang, Y.M.; Huang, J.; Zhu, X.B.; Wang, Y. Separation and recovery of sulfuric acid from acidic vanadium leaching solution by diffusion dialysis. *Sep. Purif. Technol.* **2012**, *96*, 44–49. [CrossRef]
18. Rubisov, D.H.; Papangelakis, V.G. Sulphuric acid pressure leaching of laterites-speciation and prediction of metal solubilities "at temperature". *Hydrometallurgy* **2000**, *58*, 13–26. [CrossRef]
19. Glorieux, B.; Berjoan, R.; Matecki, M.; Kammouni, A.; Perarnau, D. XPS analyses of lanthanides phosphates. *Appl. Surf. Sci.* **2007**, *253*, 3349–3359. [CrossRef]
20. Cai, Y.H.; Pan, Y.G.; Xue, J.Y.; Sun, Q.F.; Su, G.Z.; Li, X. Comparative XPS study between experimentally and naturally weathered pyrites. *Appl. Surf. Sci.* **2009**, *255*, 8750–8760. [CrossRef]
21. Deng, M.J.; Liu, Q.X.; Xu, Z.H. Impact of gypsum supersaturated solution on surface properties of silica and sphalerite minerals. *Miner. Eng.* **2013**, *46–47*, 6–15. [CrossRef]
22. Kačiulis, S.; Mattogno, G.; Pandolfi, L.; Cavalli, M.; Gnappi, G.; Montenero, A. XPS study of apatite-based coatings prepared by sol-gel technique. *Appl. Surf. Sci.* **1999**, *151*, 1–5. [CrossRef]
23. Du, J.K.; Bao, J.G.; Fu, X.Y.; Lu, C.H.; Kim, S.H. Mesoporous sulfur-modified iron oxide as an effective Fenton-like catalyst for degradation of bisphenol A. *Appl. Catal. B Environ.* **2016**, *184*, 132–141. [CrossRef]

24. Yang, X.; Zhu, M.Y.; Kang, F.F.; Cao, S.S.; Chen, R.F.; Liu, H.; Wei, Y. Formation mechanism of a series of trigonal antiprismatic jarosite-type compounds. *J. Cryst. Growth* **2015**, *429*, 49–55. [CrossRef]

25. Khoshkhoo, M.; Dopson, M.; Shchukarev, A.; Sandström, Å. Chalcopyrite leaching and bioleaching: An X-ray photoelectron spectroscopic (XPS) investigation on the nature of hindered dissolution. *Hydrometallurgy* **2014**, *149*, 220–227. [CrossRef]

26. Klauber, C. A critical review of the surface chemistry of acidic ferric sulphate dissolution of chalcopyrite with regards to hindered dissolution. *Int. J. Miner. Process.* **2008**, *86*, 1–17. [CrossRef]

27. Zhu, M.Q.; Legg, B.; Zhang, H.Z.; Gilbert, B.; Yang, R.; Banfield, J.; Waychunas, G.A. Early-stage formation of iron oxyhydroxides during neutralization of simulated acid mine drainage solutions. *Environ. Sci. Technol.* **2012**, *46*, 8140–8147. [CrossRef] [PubMed]

28. Liu, Z.H.; Brown, N.M.D.; McKinley, A. Characterisation of oxygen plasma-modified mica surfaces using XPS and AFM. *Appl. Surf. Sci.* **1997**, *108*, 319–332. [CrossRef]

29. Lim, V.W.L.; Lia, S.; Kanga, E.T.; Neoha, K.G.; Tanb, K.L. In situ XPS study of thermally deposited aluminium on chemically synthesized polypyrrole films. *Synth. Met.* **1999**, *106*, 1–11. [CrossRef]

30. Parsons, R. *Atlas of Electrochemical Equilibria in Aqueous Solutions: By Marcel Pourbaix*, 2nd ed.; Pergamon Press: Oxford, UK, 1966; pp. 234–626.

31. Yang, X.W.; He, E.P.; Yuan, B.Z. *Thermodynamics Data Calculation Manual of High Temperature Water Solution*, 1st ed.; Metallurgical Industry Press: Beijing, China, 1983; pp. 88–648.

32. Mu, W.Z.; Zhang, T.A.; Dou, Z.H.; Lü, G.Z.; Liu, Y. φ-pH diagram of V-Ti-H_2O system during pressure acid leaching of converter slag containing vanadium and titanium. *Trans. Nonferrous Met. Soc. China* **2011**, *21*, 2078–2086. [CrossRef]